

Evaluation of Dye Removal Performance of Magnetic Dendrimers with Immobilized HRP Enzyme

Nurdan Kurnaz Yetim^{1,*}, Elvan Hasanoğlu Özkan², Mümin Mehmet Koç^{3,4}

¹Kırklareli University, Faculty of Arts and Sciences, Department of Chemistry, Kırklareli, Türkiye

²Gazi University, Faculty of Sciences, Department of Chemistry, Ankara, Türkiye

³Kırklareli University, Faculty of Art and Science, Department of Physics, Kırklareli, Türkiye

⁴Kırklareli University, School of Medical Service, Kırklareli, Türkiye

In this study, magnetic nanocomposites containing polyamidoamine (PAMAM) dendrimers were synthesized and horseradish peroxidase (HRP) immobilization was carried out on this support. Then, the potential use of immobilized HRP enzyme in the decolourization of Congo red and crystal violet dyes was investigated. To determine the optimum conditions, Congo Red and Crystal Violet removal percentages were determined in the presence of free and immobilized enzyme with various parameters such as pH (3-8), temperature (20-40 °C), H₂O₂ concentration (1%-5%) and dye concentration (1.125-15 mg/L). When immobilized HRP was used, 99% decolourization was achieved for Crystal Violet after 25 minutes, while 75% decolourization was detected for Congo Red after 60 min. When we compared the immobilized and free enzyme for the decolourization of both dyes, the same removal was observed for Congo Red, while higher decolourization was observed for Crystal Violet when immobilized HRP was used.

Keywords: *Magnetic dendrimer, Fe₃O₄, PAMAM, HRP, Enzyme immobilization*

Submission Date: 28 June 2023

Acceptance Date: 12 August 2023

*Corresponding author: nurdankurnazyetim@klu.edu.tr

1. Introduction

Magnetic iron oxide nanocomposites and nanoparticles are widely used in various biomedical applications, such as drug delivery, gene delivery, protein and enzyme immobilization, hypothermia treatment of cancer [1-5]. Magnetic nanoparticles are highly susceptible to oxidation due to their superparamagnetic properties. For this reason, in order to protect the magnetic nanoparticles, a protective shell is formed on them by coating them. These shells both protect the magnetic nanoparticles and create a new magnetic nanocomposite platform that makes them more functional. A simple way to protect magnetic iron oxide nanoparticles and achieve well-defined voids is to use an organic based molecule to use as a capping agent [6-9]. Dendrimers are suitable candidates as a capping agent to

modify the surface of metal nanoparticles. They can act as structurally and chemically well-defined templates that provide good stabilization. The cavities in dendrimers are

suitable for transferring the molecules or nanoparticles contained in them to any medium [10,11]. The non-covalent interaction between guest and host is effective in such a transfer [12-14].

Magnetic nanoparticles are frequently used as support material for enzyme immobilization [15-18]. Due to the high magnetic properties of magnetic nanoparticles, they can easily be removed from the environment with the externally applied magnetic field. Thus, enzyme loss is minimized, and the immobilized enzyme can be used repeatedly. Horseradish peroxidase (HRP) enzyme is commonly used for industrial applications due to its low cost, ease of

acquisition, stability, broad substrate specificity and tolerance to wide pH and temperature ranges [19-22]. These enzymes can act on various organic molecules in the presence of hydrogen peroxide. HRP is an important enzyme used for the decolourization of aromatic amines and the treatment of wastewater, as well as for treating phenol-containing effluents [22-24]. The HRP enzyme catalyses the oxidation of various phenolic compounds by using extracellular, iron-containing molecular oxygen as an electron acceptor [25].

In this study, HRP enzyme immobilization was carried out on magnetic nanocomposite supports containing dendrimers. Free and immobilized HRP enzyme was used for the decolourization of Congo Red and Crystal Violet dyes. The removal of Congo Red and Crystal Violet in the presence of free and immobilized enzyme with many parameters like temperature, pH, amount of dye concentration and amount of H₂O₂ were investigated in order to determine the optimum conditions.

2. Experimental

2.1. Spectral data measurements

Shimadzu IR Prestige 21 was used as a FT-IR spectrometer for investigations; scanning wavenumbers were between 400 cm⁻¹ to 4000 cm⁻¹. A RIGAKU miniflex 600 X-ray diffractometer used to obtain X-ray diffraction (XRD) X-ray diffractometer was scan the sample between 10° < 2θ < 80°. SEM was used to investigate the sample surface characteristics where EDX (energy dispersive X-ray) apparatus of SEM was utilized to analyse the sample chemical composition. FEI Quanta FEG 250 model device which was equipped with EDX apparatus was used for the surface and chemical assessment. Magnetic measurements were employed at room temperature; a Cryogenic Limited PPMS-VSM (vibrating sample magnetometer) was used in the investigation. Magnetic investigation was conducted in between the magnetic field of ± 5 Tesla.

2.2. Immobilization of HRP enzyme onto magnetic PAMAM dendrimer; Fe₃O₄@G2

Magnetic PAMAM dendrimer (Fe₃O₄@G2) was synthesized following the procedure in our previous studies [5,26]. The enzyme was immobilized onto Fe₃O₄@G2 as follows: 10 mg HRP enzyme was dissolved in 10 mL of phosphate buffer solution (pH=7). The solution was then mixed with 100 mg of Fe₃O₄@G2. The new heterogeneous mixture was incubated. Incubation procedure was conducted at room temperature for 24 h. Centrifugation and washing procedures were applied three times to the

immobilized enzyme with phosphate buffer solution (PBS) (pH=7). Then the result product was dried at ambient conditions. The immobilized enzyme was kept at -4 °C in a sealed vial.

2.3. Assay of enzyme activity

The colour removal of Congo Red and Crystal Violet dyes using HRP enzyme was monitored by UV-Vis spectrophotometer. Dye decolourization rate was calculated using equation 1, where Abs(t) and Abs(i) refers the absorption of the given time and initial time, respectively.

$$D(\%) = \left(\frac{Abs(i) - Abs(t)}{Abs(i)} \right) \times 100 \quad (1)$$

For dye removal tests, 0.1 mL of free HRP enzyme solution or 2 mg of immobilized enzyme was added to 2.5 mL of buffer solution. As dye solution, 10.0 ppm (0.2 mL) Congo Red / Crystal Violet solution was used. Temperature optimization experiments were performed at 20, 30 and 40°C and optimum H₂O₂ concentration was studied using 5%, 4%, 3%, 2% and 1% (0.4 mL) H₂O₂ solutions. Dye concentration effect studies were performed using dye solutions of 15, 10, 5, 2.5 or 1.125 ppm. The degree of dye degradation was monitored by UV-spectrophotometer for 60 min. All experiments were performed in a quartz cell and the total volume was completed to 3.2 mL [24].

Name	Chemical Structure
Crystal Violet ; 4-{Bis[4-(dimethylamino)phenyl]methylidene}-N,N-dimethylcyclohexa-2,5-dien-1-iminium chloride	
Congo Red ; 3,3'-([1,1'-biphenyl]-4,4'-diyl)bis(4-aminonaphthalene-1-sulfonic acid)	

Fig.1. Structures of dyes used in colour removal

2.4. Determination of optimum pH for dye removal

0.2 mL of 10 ppm (10.0 mg/L Congo Red or Crystal Violet solutions) dye solutions were added to 2.5 mL of buffer solution at various pHs (pH 3-8). 0.1 mL HRP solution and finally 0.4 mL H₂O₂ (3%) was added to the reaction cuvette as an initiator and used for dye degradation tests.

2.5. Determination of optimum temperature for dye removal

To investigate the effect of temperature on the enzyme, the immobilized support in 2.5 mL PBS at (pH 7) was incubated in a water bath at various temperatures for 10 min and immediately used for dye degradation tests.

2.6. Determination of optimum H₂O₂ concentration for dye removal

To study the effect of H₂O₂ concentration on enzymatic decolourization, it was examined using different H₂O₂ concentrations (1%-5%) at optimum temperature and pH. The procedures in section 2.3 were repeated by varying the H₂O₂ concentration.

2.7. Determination of optimum dye concentration for dye removal

To study the effect of dye concentration on enzymatic decolourization, the optimum temperature, H₂O₂ concentration and pH were examined using different dye concentrations (1.125 ppm-15 ppm). The procedures in section 2.3 were repeated by varying the dye concentration.

3. Results

3.1. Characterization of magnetic dendrimers; Fe₃O₄@G2 and Fe₃O₄@G2@HRP

The synthesized Fe₃O₄@G2 and Fe₃O₄@G2@HRP were characterized by SEM, XRD and FT-IR analysis. Figure 2 shows the FT-IR spectra of Fe₃O₄@G2 PAMAM dendrimer and Fe₃O₄@G2@HRP. The FT-IR spectra of Fe₃O₄@G2 and Fe₃O₄@G2@HRP were similar to each other. The N-H bands groups observed at 1520 cm⁻¹ in the FT-IR spectrum of Fe₃O₄@G2 are observed at 1525 cm⁻¹ in Fe₃O₄@G2@HRP. The broad absorption band around 3300 cm⁻¹ is associated with O-H stretching. The band observed at 2933 cm⁻¹ and the band observed at 2887 cm⁻¹ wavenumbers were associated with C-H symmetric and asymmetric stretching vibrations which was attributed to alkane groups [26].

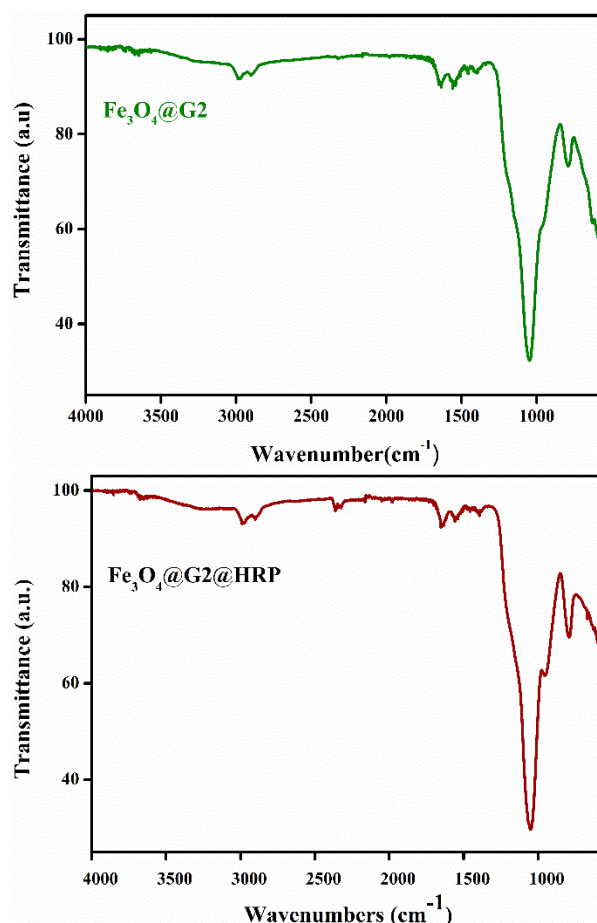


Fig.2. FT-IR spectrum of Fe₃O₄@G2 and Fe₃O₄@G2@HRP

3.2. XRD of Fe₃O₄@G2 and Fe₃O₄@G2@HRP

The XRD pattern of Fe₃O₄ magnetic nanoparticles is presented in Figure 3. When the XRD diffraction pattern is examined, the 2θ values based on the (1 1 1), (2 2 0), (3 1 1), (2 2 2), (4 0 0), (4 2 2), (5 1 1), (4 4 0), (6 2 0), (5 3 3), (6 2 2) and (4 4 4) surface-centred cubic (fcc) phase levels are 18.3°, 30.4°, 35.6°, 37.08°, 43.3°, 53.36°, 57.3°, 62.8°, 70.98°, 74.12°, 74.98° and 78.94° [27]. When the XRD pattern of dendrimer coated and enzyme immobilized magnetic dendrimer was examined, the similarity to the XRD pattern of Fe₃O₄ showed that Fe₃O₄ did not change its crystalline structure after coating and immobilization.

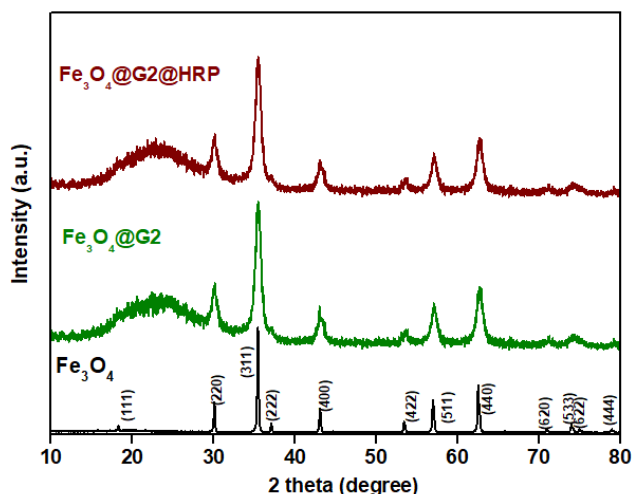


Fig.3. XRD pattern of $\text{Fe}_3\text{O}_4@\text{G2}$ and $\text{Fe}_3\text{O}_4@\text{G2}@\text{HRP}$

3.3. SEM images of $\text{Fe}_3\text{O}_4@\text{G2}$ and $\text{Fe}_3\text{O}_4@\text{G2}@\text{HRP}$

Microscopic investigations of $\text{Fe}_3\text{O}_4@\text{G2}$ and $\text{Fe}_3\text{O}_4@\text{G2}@\text{HRP}$ were performed using scanning electron microscopy (SEM) (See Figure 4). When electron microscopy images are examined, it is seen that the particles are coexisting together due to their high magnetic properties. The dendrimer coated particles were spherical and the spherical structure was preserved upon enzyme immobilization.

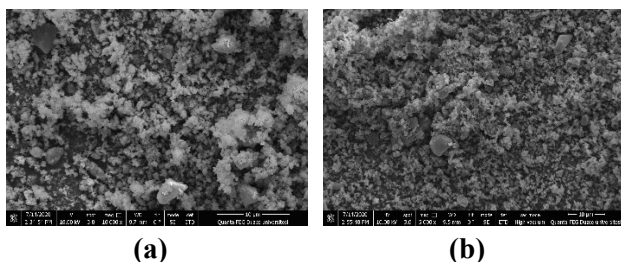


Fig.4. SEM images of (a) $\text{Fe}_3\text{O}_4@\text{G2}$, (b) $\text{Fe}_3\text{O}_4@\text{G2}@\text{HRP}$

3.4. Magnetic measurement of $\text{Fe}_3\text{O}_4@\text{G2}$ and $\text{Fe}_3\text{O}_4@\text{G2}@\text{HRP}$

The magnetic hysteresis curve of $\text{Fe}_3\text{O}_4@\text{G2}$, $\text{Fe}_3\text{O}_4@\text{G2}@\text{HRP}$ are shown in Figure 5. It was seen that magnetic $\text{Fe}_3\text{O}_4@\text{G2}$ and $\text{Fe}_3\text{O}_4@\text{G2}@\text{HRP}$ exhibit superparamagnetic characteristics. Magnetic saturation values for $\text{Fe}_3\text{O}_4@\text{G2}$, $\text{Fe}_3\text{O}_4@\text{G2}@\text{HRP}$ were found as 35.6 emu/g and 11.5 emu/g, respectively. It was observed that the magnetization decreased after enzyme immobilization on mimetic dendrimers. This supports that the immobilization process was successful.

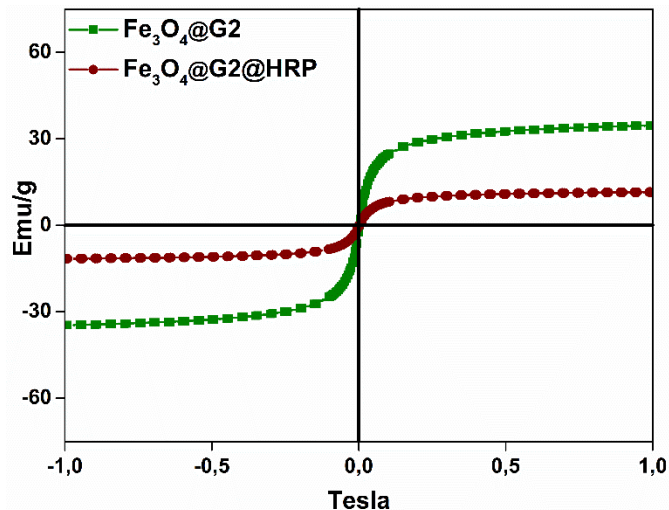
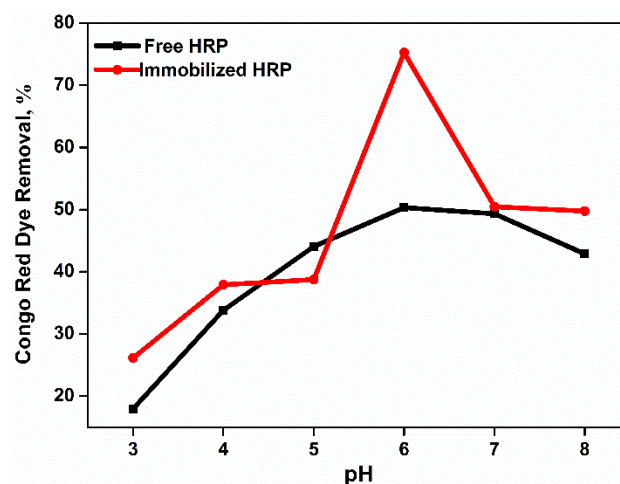


Fig.5. Magnetic hysteresis of $\text{Fe}_3\text{O}_4@\text{G2}$ and $\text{Fe}_3\text{O}_4@\text{G2}@\text{HRP}$

3.5. Decolourization of Congo Red and Crystal Violet Dyes with Free ($\text{Fe}_3\text{O}_4@\text{G2}$) and Immobilized HRP Enzyme ($\text{Fe}_3\text{O}_4@\text{G2}@\text{HRP}$)

The effect of pH on the removal of Congo Red and Crystal Violet dyes using free and immobilized HRP enzyme is presented in Figure 6. To study the pH effect on dye removal using free and immobilized enzymes, buffer solutions at various pHs (pH: 3-8) were studied. The optimum pH values for the decolourization of Congo Red dye were found to be pH:6 for free and immobilized HRP enzyme and pH:7 for Crystal Violet. When immobilized enzyme was used for Congo Red dye, 75.25% decolourization was observed at the end of one hour, while for Crystal Violet, 99.15% decolourization was recorded at 25 min. Especially at acidic pHs, the colour removal was very low.



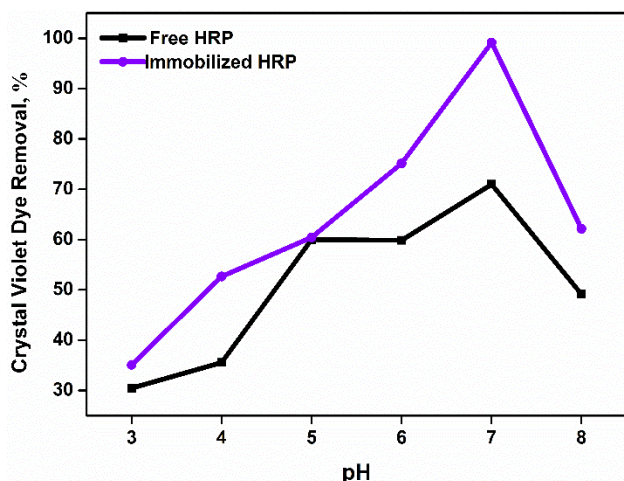


Fig. 6. Effect of pH on free and immobilized HRP catalysed a Congo Red and Crystal Violet removal

The effect of temperature on dye removal is presented in Figure 7. The highest decolourization of Congo Red and Crystal Violet dyes for free and immobilized enzyme was found to be 20°C and the efficiency decreased after this value.

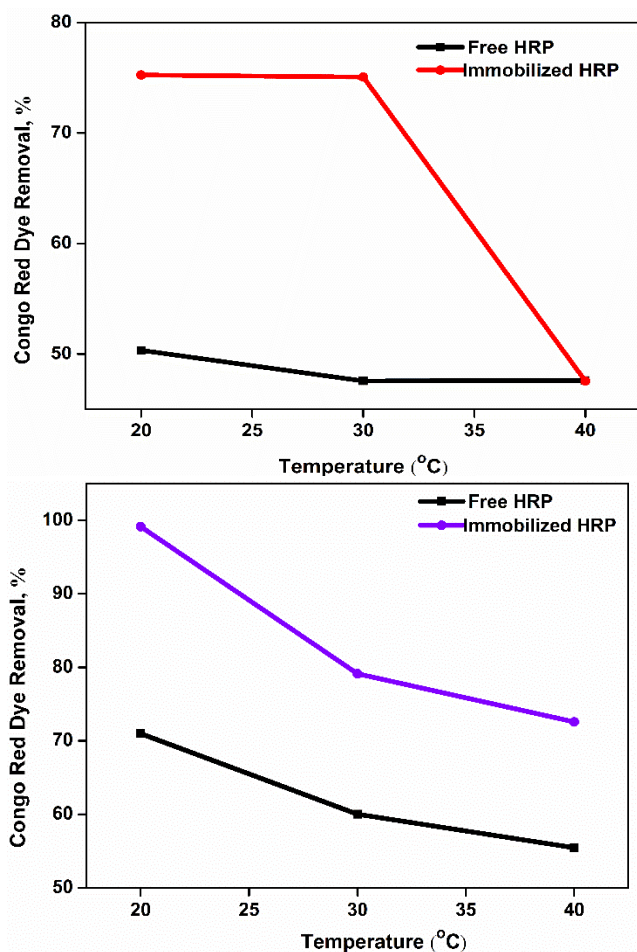


Fig. 7. Effect of temperature on free and immobilized HRP catalysed a Congo Red and Crystal Violet removal

When immobilized HRP enzyme was used, colour removal was higher than free enzyme in both dyes. The maximum colour removal for Congo Red at 20°C was 50.34% when free HRP was used and 70.98% for Crystal Violet at 20°C. When immobilized HRP was used, 75.25% and 99.15% colour removal was obtained for Congo Red and Crystal Violet, respectively.

H₂O₂ acts as a co-substrate to activate the enzymatic action of the peroxidase radical. The effect of H₂O₂ on decolourization is presented in Figure 8. In decolourization experiments using free and immobilized HRP for Congo Red and Crystal Violet, maximum decolourization was obtained at 3% H₂O₂ dose.

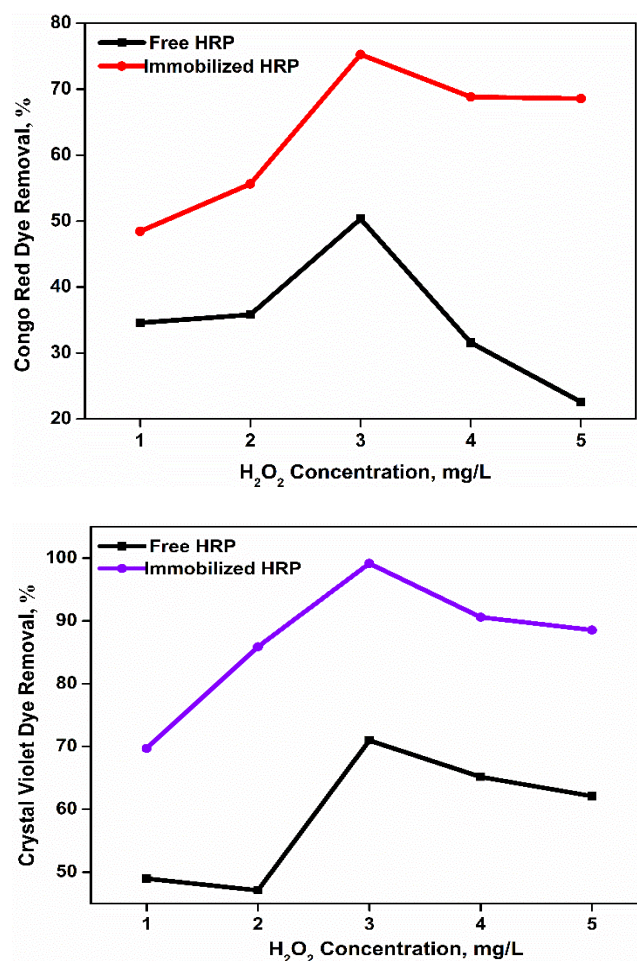


Fig. 8. Effect of H₂O₂ concentration on free and immobilized HRP catalysed a Congo Red and Crystal Violet removal

The effect of dye concentration on colour removal is studied and presented in Figure 9. While the optimum dye concentration for Congo Red dye decolourization was 10 ppm for both free and immobilized enzyme, the optimum dye concentration for Crystal Violet dye removal was 1.125 ppm for free HRP enzyme and 10 ppm for immobilized HRP enzyme. When % decolourization values were examined, for

Congo Red, both free and immobilized enzymes were used for 75% decolourization, while for Crystal Violet, 99.15% decolourization was recorded for immobilized HRP enzyme and 90.85% for free HRP enzyme.

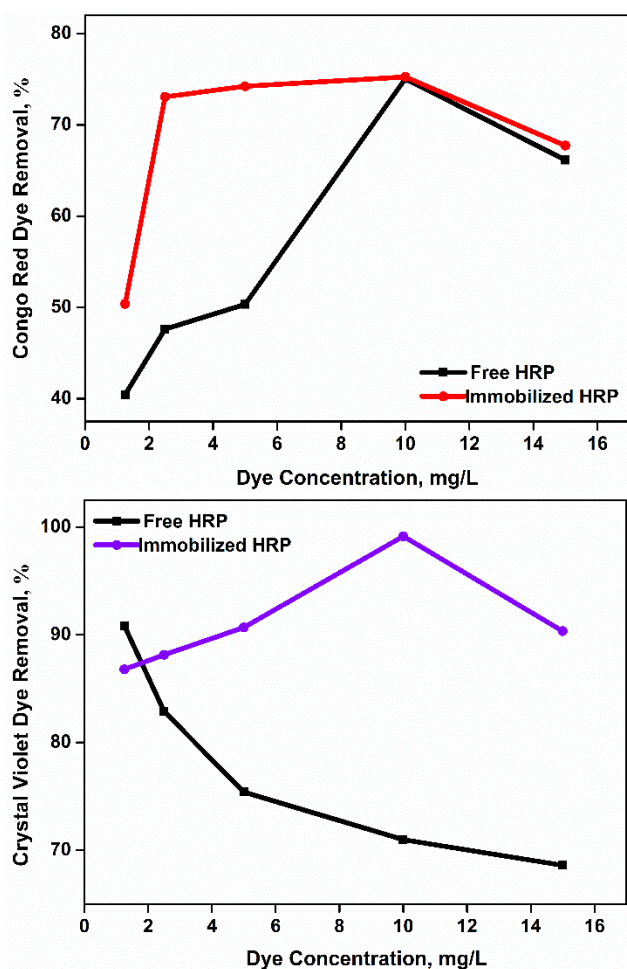


Fig. 9. Effect of dye concentration on free and immobilized HRP catalysed a Congo Red and Crystal Violet removal

4. Conclusion

From the experimental results of the study in which we examined the effect of free and immobilized HRP enzyme on the decolourization of Congo Red and Crystal Violet dyes; we can say that HRP enzyme is more effective in the decolourization of Crystal Violet dye, while it is less effective in the decolourization of Congo Red dye. When immobilized HRP was used, around 99% decolourization of Crystal Violet occurred at the end of 25 min, while 75% decolourization was detected for Congo Red after 60 min. Comparison of immobilized and free enzymes revealed that immobilized HRP could achieve decolourization while free and immobilized HRP enzyme managed to reach same decolourization rate for Congo Red.

Acknowledgements

This work was supported by Kırklareli University Scientific Research Projects Coordination Office with project numbers KLÜBAP-229 and KLÜBAP-236.

References

- [1] M. Filippousi, S.A. Papadimitriou, D.N. Bikiaris, E. Pavlidou, M. Angelakeris, D. Zamboulis, H. Tian, G. Van Tendeloo, Novel core-shell magnetic nanoparticles for taxol encapsulation in biodegradable and biocompatible block copolymers: Preparation, characterization and release properties, *Int. J. Pharm.* 448:1 (2013) 221–230. DOI: 10.1016/j.ijpharm.2013.03.025
- [2] A. Singh, S.K. Sahoo, Magnetic nanoparticles: a novel platform for cancer theranostics, *Drug Discov. Today*, 19:4 (2014) 474–481. DOI: 10.1016/j.drudis.2013.10.005
- [3] M. Sadeghi, Z. Moghimifar, H. Javadian, Fe₃O₄@SiO₂ nanocomposite immobilized with cellulase enzyme: Stability determination and biological activity, *Chem. Phys. Lett.* 811 (2023) 140161. <https://doi.org/10.1016/j.cplett.2022.140161>
- [4] R. Jin, B. Lin, D. Li, H. Ai, Superparamagnetic iron oxide nanoparticles for mr imaging and therapy: design considerations and clinical applications, *Current opinion in pharmacology*. 18 (2014) 18–27. DOI: 10.1016/j.coph.2014.08.002
- [5] N. Kurnaz Yetim, F. Kurşun Baysak, M.M. Koç, D. Nartop, Synthesis and characterization of Au and Bi₂O₃ decorated Fe₃O₄@PAMAM dendrimer nanocomposites for medical applications, *J Nanostruct. Chem.* 11 (2021) 589–599. <https://doi.org/10.1007/s40097-021-00386-w>
- [6] L. Luan, B. Tang, Y. Liu, A. Wang, B. Zhang, W. Xu, Y. Niu, Selective capture of Hg(II) and Ag(I) from water by sulfur-functionalized polyamidoamine dendrimer/magnetic Fe₃O₄ hybrid materials, *Sep. Purif. Technol.* 257 (2021) 117902. <https://doi.org/10.1016/j.seppur.2020.117902>
- [7] S. Karimia, H. Namazi, Fe₃O₄@PEG-coated dendrimer modified graphene oxide nanocomposite as a pH-sensitive drug carrier for targeted delivery of doxorubicin, *J. Alloys Compd.* 879 (2021) 160426. <https://doi.org/10.1016/j.jallcom.2021.160426>
- [8] S. Saedi, J.W. Rhim, Synthesis of Fe₃O₄@SiO₂@PAMAM dendrimer@AgNP hybrid nanoparticles for the preparation of carrageenan-based functional nanocomposite film, *Food Packag.* 24 (2020) 100473. <https://doi.org/10.1016/j.fpsl.2020.100473>
- [9] N. Kurnaz Yetim, E. Hasanoğlu Özkan, N. Akkurt, M.M. Koc, Catalytic performance of Fe₃O₄@G2-PAMAM/MoO₃ magnetic nanocomposites for degradation of 4-NP to 4-AP, *J. Mater. Electron. Device.* 3:1 (2022) 1–6.
- [10] O.C. Bodur, E. Hasanoğlu Özkan, O. Çolak, H.

- Arslan, N. Sarı, A. Dişli, F. Arslan, Preparation of acetylcholine biosensor for the diagnosis of Alzheimer's disease, *J. Mol. Struct.* 1223 (2021). <https://doi.org/10.1016/j.molstruc.2020.129168>.
- [11] F. Arslan, H. Koçak, O.C. Bodur, E. Hasanoğlu Özkan, B. Arslan, N. Sarı, Novel tyrosinase-based bisphenol-A biosensor for the determination of bisphenol-A in bracket adhesive in orthodontics, *Maced. J. Chem. Chem.* 41:2 (2022) 229-241. <https://doi.org/10.20450/mjccce.2022.2585>.
- [12] N. Kurnaz Yetim, N. Sarı, Novel dendrimers containing redox mediator: Enzyme immobilization and applications, *J. Mol. Struct.* 1191 (2019) 158-164. <https://doi.org/10.1016/j.molstruc.2019.04.09>.
- [13] E. Hasanoğlu Özkan, N. Sarı, Use of immobilized novel dendritic molecules as a marker for the detection of glucose in artificial urine, *J. Mol. Struct.* 1201 (2020) 127134. <https://doi.org/10.1016/j.molstruc.2019.127134>.
- [14] N. Kurnaz Yetim, N. Sarı, Preparation of ferrocene core dendrimers and immobilization of AChE for detection of diclofop-methyl herbicide, *Maced. J. Chem. Chem.* 38:2 (2019) 215–225. DOI: <https://doi.org/10.20450/mjccce.2019.1878>.
- [15] J. Wan, L. Zhang, B. Yang, B. Jia, J. Yang, X. Su, Enzyme immobilization on amino-functionalized Fe₃O₄@SiO₂ via electrostatic interaction with enhancing biocatalysis in sludge dewatering, *J. Chem. Eng.* 427 (2022) 131976. <https://doi.org/10.1016/j.ccej.2021.131976>.
- [16] R.M. Bezerra, R.R.C. Monteiro, D.M.A. Netob, F.F.M. da Silvaca, R.C.M. de Paulad, T.L.G. de Lemosd, P.B.A. Fachineb, M.A. Corraeae, F. Bohne, L.R.B. Gonçalvesa, J.C.S. dos Santosf, A new heterofunctional support for enzyme immobilization: PEI functionalized Fe₃O₄ MNPs activated with divinyl sulfone. Application in the immobilization of lipase from *Thermomyces lanuginosus*, *Enzyme Microb. Technol.* 138 (2020) 109560. <https://doi.org/10.1016/j.enzmictec.2020.109560>.
- [17] A. Ulu, I. Ozcan, S. Koytepe, B. Ates, Design of epoxy-functionalized Fe₃O₄@MCM-41 core-shell nanoparticles for enzyme immobilization, *Int. J. Biol. Macromol.* 115 (2018) 1122–1130. <https://doi.org/10.1016/j.ijbiomac.2018.04.15>.
- [18] J. Cuia, S. Rena, T. Linb, Y. Fengb, S. Jia, Shielding effects of Fe³⁺-tannic acid nanocoatings for immobilized enzyme on magnetic Fe₃O₄@silica core shell nanosphere, *J. Chem. Eng.* 343 (2018) 629–637. <https://doi.org/10.1016/j.ccej.2018.03.002>.
- [19] L. Razavi, H. Raissi, F. Farzad, Efficient immobilization of horseradish peroxidase enzyme on transition metal carbides, *J. Mol. Liq.* 386 (2023) 122558. <https://doi.org/10.1016/j.molliq.2023.122558>.
- [20] S.H. Cho, J. Shim, S.H. Yun, S.H. Moon, Enzyme-catalyzed conversion of phenol by using immobilized horseradish peroxidase (HRP) in a membraneless electrochemical reactor, *Appl Catal A-Gen.* 337 (2008) 66–72. doi:10.1016/j.apcata.2007.11.038.
- [21] L. Fedalto, P.R. de Oliveira, D. Agustini, C. Kalinke, C.E. Banks, M.F. Bergamini, L.H. Marcolino-Junior, Novel and highly stable strategy for the development of microfluidic enzymatic assays based on the immobilization of horseradish peroxidase (HRP) into cotton threads, *Talanta*. 252 (2023) 123889. <https://doi.org/10.1016/j.talanta.2022.123889>.
- [22] A.C. Weber, B. E. da Silva, S.G. Cordeiro, G.S. Henn, B. Costa, J.S. H. dos Santos, V.A. Corbellini, E. M. Ethur, L. Hoehne, Immobilization of commercial horseradish peroxidase in calcium alginate-starch hybrid support and its application in the biodegradation of phenol red dye, *Int. J. Biol. Macromol.* 246 (2023) 125723. <https://doi.org/10.1016/j.ijbiomac.2023.125723>.
- [23] D.A.M. Urrea, A.V. F. Gimenez, Y.E. Rodriguez, E.M. Contreras, Immobilization of horseradish peroxidase in Ca-alginate beads: Evaluation of the enzyme leakage on the overall removal of an azo-dye and mathematical modeling, *PSEP*, 156 (2021) 134–143. <https://doi.org/10.1016/j.psep.2021.10.006>.
- [24] A. Kurtuldu, H. Eşgin, N.K. Yetim, F. Semerci, Immobilization horseradish peroxidase onto UİO-66-NH₂ for biodegradation of organic dyes. *J Inorg Organomet Polym.* 32 (2022) 2901–2909. <https://doi.org/10.1007/s10904-022-02310-3>.
- [25] Y. Jiang, W. Tang, J. Gao, L. Zhou, Y. He, Immobilization of horseradish peroxidase in phospholipid-templated titania and its applications in phenolic compounds and dye removal, *Enzyme Microb. Technol.* 55 (2014) 1–6. <https://doi.org/10.1016/j.enzmictec.2013.11.005>.
- [26] N. Kurnaz Yetim, E. Hasanoğlu Özkan, M.M. Koc, Investigation of catalytic behaviour of WO₃ doped magnetic dendrimers, *Kırklareli University Journal of Engineering and Science*, 8:2 (2022) 229-242. DOI: 10.34186/klujes.1187397.
- [27] J. Safaei-Ghomi, F. Eshteghal, H. Shahbazi-Alavi, A facile one-pot ultrasound assisted for an efficient synthesis of benzo[g]chromenes using Fe₃O₄/polyethylene glycol (PEG) core/shell nanoparticles, *Ultrasonics Sonochemistry*, 33, (2016) 99-105. doi:10.1016/j.ultsonch.2016.04.025.